# Technetium-99m–Labeled *N*-(2-Hydroxypropyl) Methacrylamide Copolymers: Synthesis, Characterization, and *in Vivo* Biodistribution

**Amitava Mitra,[1] Anjan Nan,[1] Hamidreza Ghandehari,[1,2] Edwina McNeill,[3] Justin Mulholland,[3] and Bruce R. Line[2,3,4]**

*Received October 15, 2003; accepted January 2, 2004*

***Purpose.*** To synthesize novel technetium-99m ($^{99m}$Tc)-labeled *N*-(2-hydroxypropyl) methacrylamide (HPMA) copolymers and characterize the effect of charge and molecular weight on their biodistribution in SCID mice.

***Methods.*** Electronegative and neutral 7-kDa, 21-kDa, and 70-kDa HPMA copolymers containing a $^{99m}$Tc chelating comonomer, bearing N-ω-bis(2-pyridylmethyl)-L- lysine (DPK), were synthesized by free-radical precipitation copolymerization. The copolymers were labeled via $^{99m}$Tc tricarbonyl chelation to DPK-bearing comonomer. They were characterized by side-chain content, molecular weight, molecular weight distribution, radiochemical purity, and labeling stability. Scintigraphic images were obtained during the first 90 min and at 24 h postintravenous injection in SCID mice. At 24 h, organ radioactivity was determined from necropsy tissue counting.

***Results.*** $^{99m}$Tc-labeled HPMA copolymers showed greater than 90% stability over a 24-h challenge with cysteine and histidine. Scintigraphic images and the necropsy data showed that the negatively charged copolymers were eliminated from the body significantly faster than the neutral copolymers in a size-dependent manner.

***Conclusions.*** To facilitate clinical scintigraphic imaging, stable chelation of $^{99m}$Tc may be achieved by incorporation of a DPK-bearing comonomer into the HPMA backbone. Electronegative and neutral $^{99m}$Tc-labeled HPMA copolymers of 7, 21, and 70 kDa show significant variation in organ biodistribution in SCID mice. $^{99m}$Tc-labeled HPMA copolymers could be used as diagnostic agents and to study pharmacokinetics of delivery systems based on these copolymers.

**KEY WORDS:** biodistribution; drug delivery; HPMA copolymers; scintigraphic imaging; technetium-99m.

## INTRODUCTION

*N*-(2-hydroxypropyl) methacrylamide (HPMA) copolymers are a class of novel water-soluble, biocompatible, and nonimmunogenic macromolecular carrier systems that have been designed and used for the delivery of a variety of low-molecular-weight pharmaceuticals (1) as well as macromolecules (2). More than 200 different HPMA copolymers have been studied as drug carriers, and several have entered clinical trials as anticancer agents (3).

As chemotherapeutic agents based on HPMA copolymers evolve, there is a need for a clinically appropriate radiolabel to study their *in vivo* pharmacokinetics. Scintigraphic methods have been used to monitor the biodistribution of iodinated HPMA copolymers in tumor-bearing rats and mice (4,5). However, radio-iodinated compounds are not often used in patients due to suboptimal energy ($^{125}$I) and radiation dose ($^{131}$I) (6). Alternatively, technetium-99m ($^{99m}$Tc) is an ideal radiolabel to visualize the time-dependent biodistribution of drug conjugates in patients (7). A means to radiolabel HPMA with $^{99m}$Tc should facilitate translation of animal biodistribution data to patient clinical trials.

In this manuscript, we report for the first time the synthesis, characterization, and *in vivo* evaluation of $^{99m}$Tc-radiolabeled HPMA copolymers. We have studied the effect of charge and molecular weight on the biodistribution of $^{99m}$Tc-labeled HPMA copolymers up to 24 h after intravenous injection. It is apparent that both electronegative charge and molecular weight of the copolymers influence the biodistribution, body clearance rate, and the target to normal tissue background ratio of these macromolecular drug carriers.

## MATERIALS AND METHODS

### Chemicals

*N*-α-(9-fluorenylmethoxycarbonyl)-*N*-ω-bis(2-pyridylmethyl)-L-lysine [(Fmoc) DPK] was a gift from Molecular Insight Pharmaceuticals (Cambridge, MA, USA). Isolink carbonyl reaction kit was a gift from Mallinckrodt Inc. (St. Louis, MO, USA). Sodium pertechnetate was obtained from the radiopharmacy at the University of Maryland, School of Medicine (Baltimore, MD, USA) from a freshly eluted 3Ci Mallinckrodt wet column generator. All amino acids used were of L-configuration. Unless otherwise mentioned, all other chemicals were of reagent grade and obtained from Sigma Chemical Co. (St. Louis, MO, USA).

### Synthesis and Characterization of Comonomers

(Fmoc) DPK was deprotected using a previously described procedure (8). Briefly, (Fmoc) DPK was stirred in 20% piperidine/DMF for 30 min at room temperature. The resulting reaction mixture was roto-evaporated and the precipitate washed with 2:1 ether:chloroform to remove the fluvene-piperidine adduct. The deprotected DPK (DPK-$NH_2$) was dried under vacuum and was characterized using UV spectrometry ($\lambda_{max}$ = 260 nm) and mass spectrometry (MW 328).

The comonomer of *N*-methacryloylglycylglycyl-(*N*-ω-bis(2-pyridylmethyl)-L-lysine) (MA-GG-DPK) was synthesized by adding DPK-$NH_2$ in dry dimethyl sulfoxide (DMSO) to a stirred solution of *N*-methacryloylglycylglycine *p*-nitrophenyl ester (MA-GG-ONp) in DMSO in the presence of *t*-octyl pyrocatechine as inhibitor. DPK-$NH_2$ was added at a 2:1 molar excess to that of MA-GG-ONp. The reaction mixture was continuously stirred at room temperature for 24 h. The DMSO was roto-evaporated; the crude comonomer was purified by washing with ether and recrystallized from

[1] Department of Pharmaceutical Sciences, University of Maryland, Baltimore, Maryland 21201, USA.
[2] Greenebaum Cancer Center, University of Maryland, Baltimore, Maryland 21201, USA.
[3] Division of Nuclear Medicine, Department of Radiology, University of Maryland, Baltimore, Maryland 21201, USA.
[4] To whom correspondence should be addressed. (e-mail: bline@umm.edu)



0724-8741/04/0700-1153/0 © 2004 Plenum Publishing Corporation

methanol. The comonomer was dried under vacuum and characterized using UV spectrometry ($\lambda_{max}$ = 260 nm, $\varepsilon$ = 5662.3 $M^{-1}cm^{-1}$) and mass spectrometry (MW 510).

All other comonomers, namely, HPMA (MP 66–68°C) (9), *N*-methacryloylglycylglycine (MA-GG-COOH) (MP 195–199°C) (10), and *N*-methacryloyltyrosinamide (MA-Tyr) (MP 194–196°C) (11) were synthesized according to previously described methods.

### Synthesis and Characterization of HPMA Copolymers

The neutral and electronegative HPMA copolymers were synthesized by free-radical precipitation copolymerization in acetone/DMSO using *N, N′*-azobisisobutyronitrile (AIBN) (Sigma) as the initiator. The molar feed composition of the comonomers for the neutral and electronegative copolymers are shown in Table I. The comonomer mixtures were sealed in an ampoule under nitrogen and stirred at 50°C for 24 h. The precipitated copolymer was dissolved in methanol and reprecipitated in acetone:ether (3:1) to obtain the pure product. Copolymer MA-GG-DPK and MA-Tyr content were determined by amino acid analysis, and MA-GG-COOH content was assessed by acid–base titration (12). Weight average molecular weight and molecular weight distribution (polydispersity) were estimated by size exclusion chromatography on a Superose 12 column (10 mm × 30cm) (Pharmacia, Piscataway, NJ, USA) using a fast protein liquid chromatography (FPLC) system (Pharmacia). Copolymer fractions were selected with molecular weights (7 kDa and 21 kDa) below the renal threshold of glomerular filtration (~45 kDa), and one fraction was obtained above (70kD) the threshold. Copolymer fractions were obtained by elution on a Superose 12 preparative column (16 mm × 50 cm), using PBS (pH 7.4). The fractions were then dialyzed against distilled water and lyophilized.

### $^{99m}$Tc Radiolabeling and Challenge Studies with Cysteine and Histidine

The HPMA copolymer fractions were radiolabeled using a two-step procedure (Isolink kit carbonyl reaction, Mallinckrodt). First, $^{99m}$Tc-tricarbonyl [$^{99m}Tc(H_2O)_3(CO)_3$] (Fig. 1a) was synthesized by adding 1 ml of sodium pertechnetate ($NaTcO_4$) to a Isolink carbonyl reaction vial (Mallinckrodt) containing lyophilized sodium tartarate, sodium borate, sodium carbonate, and sodium boranocarbonate. The resulting solution was then placed in a boiling water bath for 20 min. Second, 120 μl of 1 N hydrochloric acid was added to neutralize the solution and decompose any residual boranocarbonate. Two hundred microliters of the polymer solution was added, and the mixture was heated for 30 min at 75°C. The labeled copolymers were purified over a Sephadex G-25 column (PD-10 desalting column, Amersham Biosciences, Piscataway, NJ, USA) using normal saline.

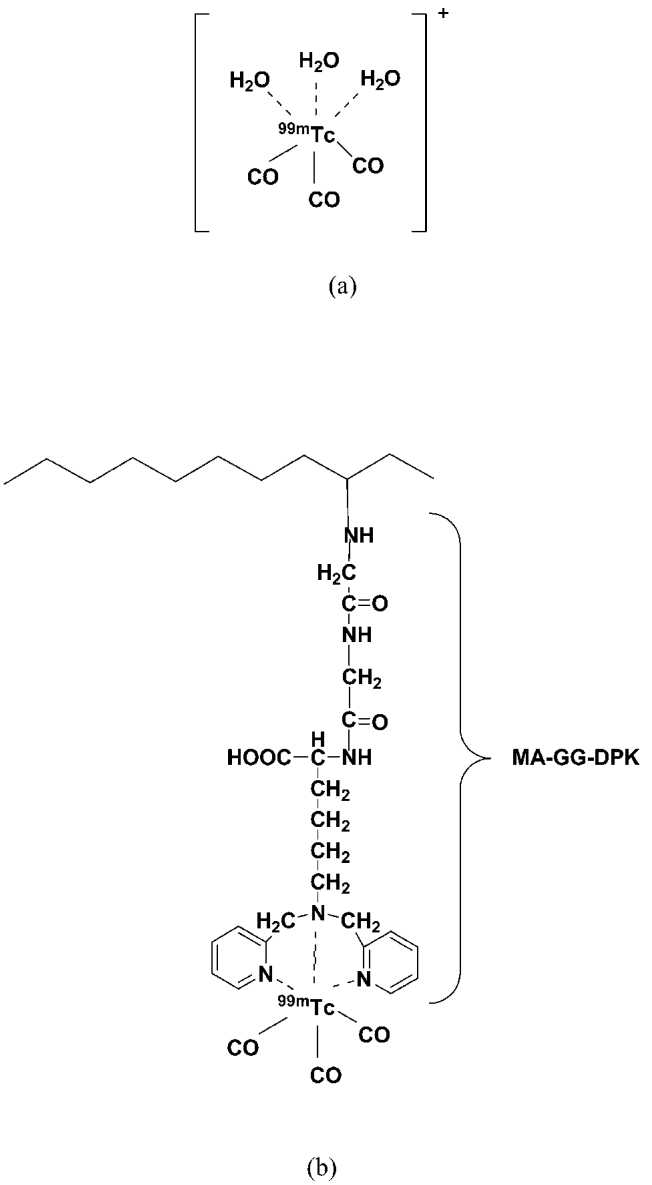


**Fig. 1.** (a) Structure of $^{99m}$Tc-tricarbonyl [$^{99m}Tc(H_2O)_3(CO)_3$] and (b) schematic of $^{99m}$Tc-labeled HPMA copolymer containing the chelating comonomer MA-GG-DPK. The comonomer MA-GG-DPK was used to label the copolymer backbone with $^{99m}$Tc-tricarbonyl.

Solutions of 1 mM cysteine and 1 mM histidine in PBS (pH 7.4) were added to aliquots of the $^{99m}$Tc-labeled HPMA copolymer (Fig. 1b) (final ligand concentration, $10^{-6}$ M). The samples were incubated at 37°C, and the retained copolymer

**Table I.** Feed Composition of Comonomers in Neutral and Electronegative HPMA Copolymers

| Sample | Feed composition of comonomers (mol%)* | | | |
|---|---|---|---|---|
| | HPMA | MA-GG-DPK | MA-GG-COOH | MA-Tyr |
| Neutral copolymer | 95 | 5 | — | — |
| Electronegative copolymer | 70 | 5 | 23 | 2 |

* 12.5 wt% comonomers dissolved in acetone/DMSO.

**Table II.** Physicochemical Characteristics of Neutral and Electronegative HPMA Copolymer Fractions

| | Neutral copolymer | | | Electronegative copolymer | | |
|---|---|---|---|---|---|---|
| | 7 kDa | 21 kDa | 70 kDa | 7 kDa | 21 kDa | 70 kDa |
| DPK content (mmol/g polymer)* | 0.2678 | 0.2705 | 0.2785 | 0.2146 | 0.2155 | 0.2171 |
| COOH content (mmol/g polymer)† | — | — | — | 0.952 ± 0.005 | 1.023 ± 0.004 | 1.02 ± 0.004 |
| Tyr content (mmol/g polymer)* | — | — | — | 0.066 | 0.064 | 0.071 |
| Actual $M_w$ (kD)‡ | 7.9 | 22.1 | 72.2 | 8.3 | 23 | 74.1 |
| Polydispersity‡ | 1.1 | 1.2 | 1.3 | 1.2 | 1.3 | 1.3 |

* Results of amino acid analysis.
† Results of acid-base titration. Values represent the means ± SD (n = 3).
‡ As determined by size exclusion chromatography.

activity was measured in a dose calibrator (Capintec, Ramsey, NJ, USA) after Sephadex G-25 column isolation at 5 min, 1, 4, and 24 h. Student's unpaired *t* test was performed to determine statistical significance of the differences in the observed displacement of $^{99m}$Tc from the copolymer backbone after 24 h.

### Imaging and Biodistribution Studies

Four- to 5-week old male Harlan Sprague-Dawley SCID mice (average weight, 25 g) were studied under the University of Maryland Institutional Animal Care and Use Committee (IACUC) approved protocol. All animals were anesthetized (13) and injected via the lateral tail vein with 200 μl of normal saline containing 25 nmol of $^{99m}$Tc-labeled HPMA (300–400 μCi). To assess the early organ biodistribution, a dynamic 90-min image was obtained immediately after intravenous injection using a dual head gamma camera with a low-energy, all-purpose collimator (DSX-LI, SMV, Berlin, Germany).

At 24 h, a 30-min scintigraphic image was obtained to evaluate residual organ activity, and orbital blood samples were obtained. During necropsy, whole organ tissue samples were obtained from the heart, lung, liver, spleen, kidney, and muscle. The tissue samples were washed with water, counted (Cobra II Autogamma, Packard, Meriden, CT, USA), weighed, and the percentage-injected dose per gram tissue (%ID/g) was calculated. All biodistribution studies were performed with 5 mice per group. Student's unpaired *t* test was performed to determine statistical significance of the observed differences in organ accumulation between the neutral and electronegative copolymer fractions. One-way ANOVA test was used to determine statistical significance of the differences in the organ accumulation between the molecular weight fractions of the neutral and electronegative copolymers.

## RESULTS

The side-chain content, molecular weight, and molecular weight distribution characteristics of the copolymer fractions are shown in Table II. The weight average molecular weights of the unfractionated copolymers as estimated by size exclusion chromatography were 86 kDa and 60.1 kDa for the neutral and electronegative copolymers, respectively. The estimated weight average molecular weights ($M_w$) of the copolymer fractions are listed in Table II, but for simplification they are named as 7-, 21-, and 70-kDa copolymers. Upon fractionation the 7-, 21-, and 70-kDa copolymers showed narrow polydispersity (1.1–1.3) for both the neutral and electronegative species. The polydispersity ($M_w/M_n$) of the copolymers were consistent with the previously reported data for HPMA copolymers (14). The DPK, COOH, and tyrosinamide contents were consistent with their corresponding feed compositions during polymerization. The DPK content averaged 83% and 89% of the feed composition for the neutral and electronegative fractions, respectively.

The copolymers were labeled by $^{99m}$Tc-tricarbonyl-DPK chelation (Fig. 1b). Typically, specific activities greater than 16 mCi/mg (12.5 MBq/nM) were obtained with a radiolabeling efficiency of greater than 92%. The challenge studies with cysteine and histidine (Table III) showed excellent $^{99m}$Tc binding stability over 24 h with less than 10% displacement (statistically insignificant) from the polymer backbone. There was a slightly higher $^{99m}$Tc displacement in the presence of excess histidine.

The SCID mouse images showed a clear difference in the

**Table III.** Stability of Complexes (%)* Against Ligand Exchange in Excess Histidine and Cysteine in Phosphate-Buffered Saline at 37°C

| | Histidine (1 mM) | | | | Cysteine (1 mM) | | | |
|---|---|---|---|---|---|---|---|---|
| Samples | 5 min | 1 h | 4 h | 24 h | 5 min | 1 h | 4 h | 24 h |
| Neutral copolymer | 97.98 ± 0.65 | 95.79 ± 1.1 | 94.48 ± 0.98 | 90.11 ± 1.4 | 98.32 ± 0.97 | 96.79 ± 1.12 | 96.55 ± 0.89 | 93.68 ± 0.58 |
| Electronegative copolymer | 98.35 ± 0.31 | 95.09 ± 0.58 | 93.92 ± 1.19 | 90.96 ± 1.8 | 98.71 ± 1.1 | 97.23 ± 0.59 | 96.97 ± 1.5 | 94.27 ± 1.2 |

* Values represent the means ± SD (n = 3).

copolymer biodistribution patterns at 90 min post injection (Fig. 2). The electronegative copolymers were largely confined to the blood pool, kidney, and bladder regions. The 70-kDa copolymer fraction persisted in the thoracic region, whereas little chest activity was evident for the 7- and 21-kDa fractions. All of the electronegative copolymers were evident in the kidney and bladder region with a pattern consistent with their relative sizes. The 21-kDa fraction transited the kidney more slowly than the 7-kDa fraction, which was largely found in the bladder by 90 min postinjection. There did not appear to be a significant concentration of the electronegative copolymers in either the liver or the spleen.

The neutral copolymers also showed a pattern of renal clearance that was related to molecular weight. The 7-kDa fraction largely passed into the bladder by 90 min, whereas the 70-kDa fraction showed a relatively small clearance. For a given weight, the neutral copolymers appeared to clear the body at a slower rate than the electronegative copolymers. Furthermore, there appeared to be more localization of the neutral polymers in the region of the liver and spleen at 90 min post dose.

The 24-h necropsy radioactivity in tissues was expressed as percent of the injected dose per gram tissue (%ID/g) (Figs. 3 and 4). The neutral 7-kDa copolymer fraction (Fig. 3) persisted primarily in the liver (5.3 ± 1.7% ID/g) and spleen (5.9 ± 1.9%). The 21-kDa fraction cleared from all the organs except for the kidney (18.3 ± 6.9%) and spleen (10.3 ± 1.3%). The 70-kDa fraction showed high blood activity (19.2 ± 4.2%) and the highest 24 h copolymer localization in lung (12.8 ± 3.1%), spleen (14.9 ± 4.5%), and liver (25.3 ± 2.8%).

The electronegative copolymers (Fig. 4) cleared well from all tissues with the 7-kDa fraction showing trace quantities in the kidney (8.1 ± 0.74%). Higher renal activity was found for the 21-kDa and 70-kDa fractions, which showed 33.1 ± 1.6% and 23.3 ± 4.8%, respectively. The 70-kDa fraction showed small quantities in the blood (1.5 ± 0.3%), spleen (1.4 ± 0.7%), and liver (2.2 ± 0.6%).

The comparison of the absolute amounts of radioactivity in the organs (%ID/g) for the neutral and electronegative copolymers is shown in Table IV. There was a significant difference ($p < 0.05$) in organ accumulation between neutral and electronegative copolymer fractions of similar molecular weight, with the neutral copolymer fractions showing higher organ accumulation than electronegative copolymer fractions. The kidney accumulation was, however, significantly higher for the electronegative fractions as compared to the neutral fractions. Similarly, there was significant difference ($p < 0.05$) in organ accumulation among the different molecular weight fractions for both the neutral and electronegative copolymers except for neutral 7-kDa and 21-kDa fractions in the liver.

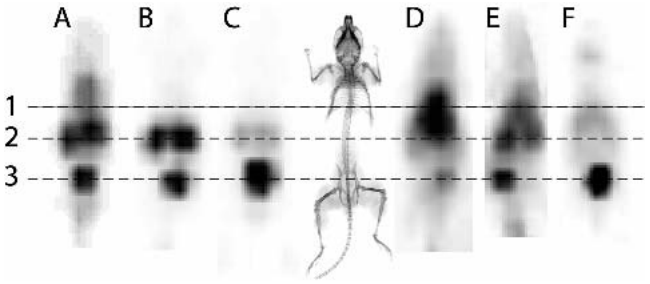


**Fig. 2.** Scintigraphic images of SCID mice, 90 min after intravenous injection of electronegative (A, 70 kDa; B, 21 kDa; C, 7 kDa) and neutral (D, 70 kDa; E, 21 kDa; F, 7 kDa) $^{99m}$Tc-HPMA copolymer fractions. The markers 1, 2, and 3 are used to indicate heart, kidney, and bladder regions, respectively. The region between 1 and 2 represents liver. After 90 min, the electronegative fractions show significant localization in kidney and bladder indicating rapid excretion from the body. Of the neutral fractions, only 7 kDa shows bladder localization after 90 min, and the 70 kDa is largely taken up by the liver due to reduced glomerular filtration.

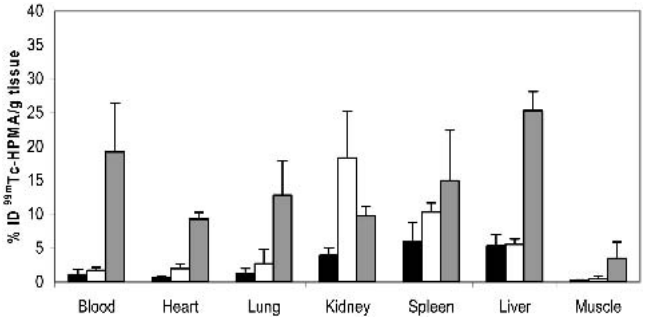


**Fig. 3.** Residual radioactivity in % injected dose per gram of organ tissue 24 h after injection of neutral $^{99m}$Tc-HPMA copolymer fractions. The excised organs were counted using a gamma counter; data are expressed as mean ± SD (number of animals/group is shown). Key: ■ 7 kDa (n = 5), □ 21 kDa (n = 5), ▩ 70 kDa (n = 4).

## DISCUSSION

Long-chain macromolecules such as HPMA copolymers have been used as carriers of drugs to enhance their stability *in vivo* and as targeted delivery systems. Low-molecular-weight anticancer agents, for example, show improved therapeutic activity when conjugated to copolymers of HPMA (15). Because the biodistribution of such drug conjugates is influenced by the properties of the carrier system, we developed a $^{99m}$Tc-radiolabeled copolymer of HPMA to evaluate these properties *in vivo*.

$^{99m}$Tc is eluted in saline solution from a $^{99}$Mo/$^{99m}$Tc generator as sodium pertechnetate. In preparation of radiopharmaceuticals, the technetium (+7) in pertechnetate is reduced to a lower oxidation state for ligand coordination. Alberto *et*

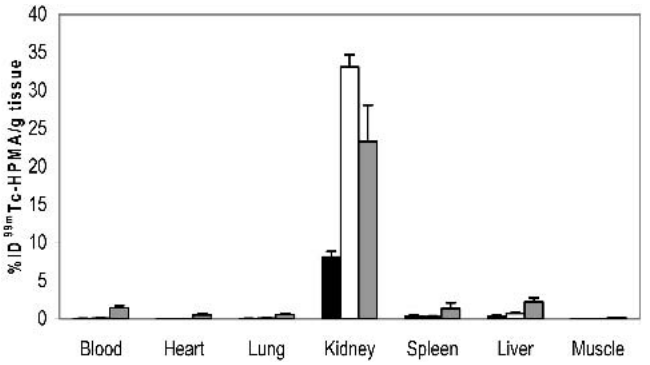


**Fig. 4.** Residual radioactivity in % injected dose per gram of organ tissue 24 h after injection of electronegative $^{99m}$Tc-HPMA fractions. The excised organs were counted using a gamma counter; data are expressed as mean ± SD (number of animals/group is shown). Key: ■ 7 kDa (n = 5), □ 21 kDa (n = 5), ▩ 70 kDa (n = 5).

**Table IV.** Percent Injected Dose per Gram Organ Tissue (%ID/g)* at 24 Hours for Neutral and Electronegative HPMA Copolymers

| | Neutral copolymer | | | Electronegative copolymer | | |
|---|---|---|---|---|---|---|
| | 7 kDa | 21 kDa | 70 kDa | 7 kDa | 21 kDa | 70 kDa |
| Blood | 1.1 ± 0.3 | 1.7 ± 0.5 | 19.2 ± 4.2 | 0.048 ± 0.006 | 0.084 ± 0.02 | 1.454 ± 0.25 |
| Heart | 0.6 ± 0.1 | 2.0 ± 0.7 | 9.3 ± 1.0 | 0.028 ± 0.005 | 0.035 ± 0.006 | 0.518 ± 0.13 |
| Lung | 1.3 ± 0.4 | 2.7 ± 1.1 | 12.8 ± 3.1 | 0.049 ± 0.008 | 0.071 ± 0.03 | 0.542 ± 0.17 |
| Kidney | 3.9 ± 1.1 | 18.3 ± 6.9 | 9.7 ± 1.4 | 8.137 ± 0.74 | 33.104 ± 1.59 | 23.277 ± 4.8 |
| Spleen | 5.9 ± 1.9 | 10.3 ± 1.3 | 14.9 ± 4.5 | 0.387 ± 0.17 | 0.284 ± 0.13 | 1.361 ± 0.72 |
| Liver | 5.3 ± 1.7 | 5.5 ± 0.8 | 25.3 ± 2.8 | 0.382 ± 0.17 | 0.716 ± 0.076 | 2.208 ± 0.56 |
| Muscle | 0.2 ± 0.1 | 0.5 ± 0.1 | 3.5 ± 2.4 | 0.031 ± 0.02 | 0.032 ± 0.01 | 0.129 ± 0.02 |

* Values represent the means ± SD (n = 5, except for 70-kDa neutral copolymer, where n = 4).

*al.* recently developed one of the most stable technetium chelates in the form of $^{99m}$Tc-tricarbonyl [$^{99m}Tc(H_2O)_3(CO)_3$] (16) (Fig. 1a). The technetium at the complex center is very inert chemically given its low oxidation state (+1) and its carbonyl protected spherical shape, which protects the technetium from further ligand attack or reoxidation (17). This $^{99m}$Tc-tricarbonyl core forms very stable complexes with tridentate ligands by replacing the three coordinated water molecules (18,19) (Fig. 1b).

Instability of $^{99m}$Tc radiolabeled HPMA *in vivo* can occur through two principal routes: through proteolytic degradation of the peptide side chain by serum proteases or by transchelation of the technetium to other high-affinity binding sites. *N*-ω-bis(2-pyridylmethyl)-L-lysine (DPK) was chosen to form the $^{99m}$Tc binding comonomer as it provides a compact tridentate coordination that should resist proteolytic attack. The [DPK-$^{99m}Tc(CO)_3$] (Fig. 1b) complex offers no free coordination site for attack by competing ligands (20). As technetium shows a high affinity for sulfur-containing molecules, its tendency to transchelate *in vivo* can be modeled *in vitro* by challenge with cysteine (21). Histidine challenge is used as a means to test the coordination efficiency of DPK toward the metal center of $^{99m}Tc(H_2O)_3(CO)_3$ (18). The comonomer of the tridentate ligand (DPK) was observed to coordinate strongly with the tricarbonyl core showing excellent stability in cysteine and histidine challenges. In the HPMA copolymers synthesized in this work, approximately five DPK units were incorporated in each polymer chain. This is far in excess of the number of DPK units required to coordinate the $^{99m}$Tc label. In the animal experiments, for example, each animal received 25 nmol of HPMA radiolabeled with about 350 μCi. This translates to about 4000 DPK for every $^{99m}$Tc atom coordinated, an excess that facilitates rapid polymer labeling.

HPMA copolymers are loosely coiled macromolecules, which are slowly captured by fluid phase pinocytosis (22). We studied the fate and the total body distribution of $^{99m}$Tc-HPMA copolymers (MW 7 kDa, 21 kDa, and 70 kDa) in SCID mice over 24 h. As expected, the renal elimination rate of intravenously injected HPMA copolymers was dependent on molecular weight and charge, with the charge having the predominant effect on biodistribution (4,14,23,24).

Images obtained at 90 min of the *in vivo* biodistribution of the neutral and electronegative HPMA copolymers are clearly different for each of the molecular weights and for the molecular charges.

At 90 min, the neutral $^{99m}$Tc-HPMA copolymers demonstrate progressively less tissue activity for the 70-, 21-, and 7-kDa copolymers. The highest uptake of the neutral 70-kDa fraction was seen in lung, liver, and spleen, which was consistent with previously published data (4).

The electronegative copolymers do not appear to be taken up to a significant extent by any body organ other than the kidneys. The scintigraphic images and the 24-h necropsy data show that the negatively charged copolymer fractions are more efficiently cleared from the body than the neutral copolymers. All the neutral compounds show hepatic activity, whereas little liver uptake was evident for the electronegative copolymer fractions. These findings may be due, in part, to reduced transvascular flux from repulsion of the electronegative copolymers by negatively charged plasma membranes (23).

At 24 h, the retention of neutral HPMA in necropsy tissue is closely related to copolymer molecular weight. For all nonrenal tissues (heart, lung, spleen, liver, and muscle), the higher the molecular weight, the higher the tissue radioactivity. It is well established that following IV administration, smaller (<45 kDa) HPMA neutral copolymer fractions are subject to rapid renal clearance, but the higher molecular weight (70 kDa) fraction persists in the blood for prolonged period as it falls above the renal glomerular filtration threshold (45 kDa) for HPMA (14,24).

Radioiodinated HPMA has been used to study the biodistribution and the cellular localization of HPMA (4,5). Kissel *et al.* studied the time-dependent distribution of $^{131}$I-labeled HPMA in whole-body scintigraphy of tumor-bearing animals over 7 days. They demonstrated the relationship between copolymer molecular weight and plasma circulation time, body excretion, and tumor localization of HPMA (4). Copolymers were cleared from the blood in a molecular-weight–dependent manner, either via excretion or by extravasation into normal and neoplastic tissues. The higher the molecular weight, the greater the radioactivity taken up by organ tissues. As with the neutral $^{99m}$Tc-radiolabeled copolymers, highest amounts were accumulated in the lung, liver, and spleen. Kissel *et al.* showed that the kinetics of HPMA accumulation in solid tumors was also dependent on copolymer molecular weight. HPMA copolymers with molecular weights below the renal threshold peaked in tumor tissue at 24 h postinjection and then remained constant. In contrast, copolymers above the renal clearance threshold displayed continuous accumulation and significantly higher tumor uptake (4).

Despite the utility of radio-iodinated HPMA conjugates

in animal model studies, it has serious shortcomings in clinical use. $^{131}I$ is generally not used for diagnostic imaging because of its high gamma energy (364 keV) and the radiation dose associated with its beta emission. $^{125}I$ produces low-energy gamma emissions (80 keV) with low tissue penetration that limits its use in man. $^{123}I$, the most suitable iodine isotope for clinical imaging, is short lived ($t_{1/2}$ = 13.3 h) and relatively expensive because it is cyclotron produced. The radiolabeling and distribution logistics associated with $^{123}I$ make it less attractive for clinical use (6). The preferred isotope is $^{99m}Tc$ because of its wide availability, ideal imaging energy (140 keV), and lack of beta emission. It is the radionuclide used in more than 80% of all diagnostic nuclear medicine procedures (7).

The ability to radiolabel HPMA with $^{99m}Tc$ and to modulate copolymer molecular weight and charge opens many possibilities for use of these compounds in diagnosis and targeted therapy. Shorter molecules may be suitable to study the patterns of lymph flow in a manner similar to $^{99m}Tc$-radiolabeled dextran (25). $^{99m}Tc$-labeled HPMA copolymers bearing peptide ligands for the $\alpha_v\beta_3$ integrin on neovascular endothelial cells may provide a means to detect sites of cancer or may be useful in assessing the efficacy of angiogenesis inhibitors (26,27). Incorporation of negative charge on the copolymer appears to significantly reduce organ uptake. Specific targeting to tumor sites and low extravasation into normal tissues could result in enhanced tumor/background distribution of a polymer-drug conjugates.

## CONCLUSIONS

The biodistribution of neutral and electronegative HPMA copolymers have been studied using $^{99m}Tc$ gamma scintigraphy in SCID mice. Stable $^{99m}Tc$ complexes have been formed with HPMA copolymers by incorporating comonomers bearing *N*-ω-bis(2-pyridylmethyl)-L-lysine (DPK) into the polymeric backbone. The tissue biodistribution and renal elimination rate of $^{99m}Tc$-radiolabeled HPMA copolymers is dependent on both molecular weight and charge. Our work suggests that $^{99m}Tc$-radiolabeled HPMA copolymers will provide a means to carry out human imaging studies to assess the pharmacokinetics of HPMA copolymers as carriers for diagnostic and therapeutic agents.

## ACKNOWLEDGMENTS

The authors would like to thank Dr. John W. Babich of Molecular Insight Pharmaceuticals for providing DPK and Dr. Mary Dyszlewski of Mallinckrodt Inc. for providing Isolink carbonyl reaction kit. The authors appreciate the help of Alvin Jumpp and Tomika Coleman with the animal studies and Kristin Lanham with the imaging experiments. This research was supported by NIH grants CA 99-015 and 98-008.

## REFERENCES

1. J. Kopecek, P. Kopeckova, T. Minko, and Z. R. Lu. HPMA copolymer-anticancer drug conjugates: design, activity and mechanism of action. *Eur. J. Pharm. Biopharm.* **50**:61–81 (2000).
2. Z.-R. Lu, J-G Shiah, S. Sakumma, P. Kopeckova, and J. Kopecek. Design of novel bioconjugates for targeted drug delivery. *J. Control. Rel.* **78**:165–173 (2002).
3. R. Duncan. The dawning era of polymer therapeutics. *Nat. Rev. Drug Discov.* **2**:347–360 (2003).
4. M. Kissel, P. Peschke, V. Subr, K. Ulbrich, J. Schuhmacher, J. Debus, and E. Friedrich. Synthetic macromolecular drug carriers: biodistribution of poly [(N-2-hydroxypropyl) methacrylamide] copolymers and their accumulation in solid rat tumors. *PDA J. Pharm. Sci. & Tech.* **55**:191–201 (2001).
5. M. V. Pimm, A. C. Perkins, J. Strohalm, K. Ulbrich, and R. Duncan. Gamma scintigraphy of $^{123}I$ labeled N-(2-hydroxypropyl) methacrylamide copolymer doxorubicin conjugate containing galactosamine following intravenous administration to nude mice bearing hepatic human colon carcinoma. *J. Drug Targ.* **3**:385–390 (1996).
6. A. J. Fischman, J. W. Babich, and H. W. Strauss. A ticket to ride: peptide radiopharmaceuticals. *J. Nucl. Med.* **34**:2253–2263 (1993).
7. S. Banerjee, M. R. A. Pillai, and N. Ramamoorthy. Evolution of Tc-99m in diagnostic radiopharmaceuticals. *Sem. Nuc. Med.* **31**: 260–277 (2001).
8. G. B. Fields and R. L. Nobel. Solid phase peptide synthesis utilizing 9-fluorenylmethoxycarbonyl amino acids. *Intl. J. Peptide Protein Res.* **35**:161–214 (1990).
9. J. Strohalm and J. Kopecek. Poly N-(2-hydroxypropyl) methacrylamide. 4. Heterogeneous polymerization. *Angew. Makromol. Chem.* **70**:109–118 (1978).
10. P. Rejmanova, J. Labsky, and J. Kopecek. Aminolysis of monomeric and polymeric *p*-nitrophenyl esters of methacryloylated amino acids. *Macromol. Chem.* **178**:2159–2168 (1977).
11. J. H. Lee, P. Kopeckova, J. Kopecek, and J. D. Andrade. Surface properties of copolymers of alkyl methacrylates with, methoxy (polyethylene oxide) methacrylates and their application as protein-resistant coatings. *Biomaterials* **11**:455–464 (1990).
12. P. Y. Yeh, P. Kopeckova, and J. Kopecek. Biodegradable and pH sensitive hydrogels: Synthesis by crosslinking of N,N-dimethylacrylamide copolymer precursors. *J. Polym. Sci: Part A. Polym. Chem.* **32**:1627–1637 (1994).
13. V. E. Papaioannou. Efficacy of tribromoethanol anesthesia in mice. *Lab. Anim. Sci.* **43**:189–192 (1993).
14. L. W. Seymour, Y. Miyamoto, H. Maeda, M. Brereton, J. Strohalm, K. Ulbrich, and R. Duncan. Influence of molecular weight on passive tumor accumulation of a soluble macromolecular drug carrier. *Eur. J. Cancer* **31A**:766–770 (1995).
15. P. S. Steyger, D. F. Baban, M. Brereton, K. Ulbrich, and L. W. Seymour. Intratumoural distribution as a determinant of tumour responsiveness to therapy using polymer-based macromolecular prodrugs. *J. Control. Rel.* **39**:35–46 (1996).
16. R. Alberto, R. Schibli, A. Egli, A. P. Schubiger, U. Abram, and T. A. Kaden. A novel organometallin aqua complex of technetium for the labeling of biomolecules: synthesis of $[^{99m}Tc(H_2O)_3(CO)_3]^+$ from $[^{99m}TcO_4]^-$ in aqueous solution and its reaction with a bifunctional ligand. *J. Am. Chem. Soc.* **120**: 7987–7988 (1998).
17. R. Schibli and P. A. Schubiger. Current use and future potential of organometallic radiopharmaceuticals. *Eur. J. Nucl. Med.* **29**: 1529–1542 (2002).
18. R. Schibli, R. La Bella, R. Alberto, E. G. Garayoa, K. Ortner, U. Abram, and P. A. Schubiger. Influence of the denticity of ligand systems on the in vitro and in vivo behavior of (99m)Tc(I)-tricarbonyl complexes: A hint for the future functionalization of biomolecules. *Bioconjug. Chem.* **11**:345–351 (2000).
19. R. Schibli, K. V. Katti, C. Higginbotham, W. A. Volkart, and R. Alberto. In vitro and in vivo evaluation of bidentate water soluble phosphine ligands as anchor groups for the organometallic fac-$^{99m}Tc(CO)_3$ core. *Nucl. Med. Biol.* **26**:711–716 (1999).
20. A. Egli, R. Alberto, L. Tannahill, R. Schibli, U. Abram, A. Schaffland, R. Waibel, D. Tourwe, L. Jeannin, K. Iterbeke, and P. A. Schubiger. Organometallic 99mTc- aquaion labels peptide to an unprecidented high specific activity. *J. Nucl. Med.* **40**:1913–1917 (1999).
21. M. A. Stalteri, S. Bansal, R. Haider, and S. J. Mather. Comparison of the stability of technetium labeled peptides to challenge with cysteine. *Bioconjugate Chem.* **10**:130–136 (1999).

22. D. Putnam. and J. Kopecek. Polymer conjugates with anticancer activity. *Adv. Polymer Sci.* **122**:55–123 (1995).
23. M. Kissel, P. Peschke, V. Subr, K. Ulbrich, J. Schuhmacher, J. Debus, and E. Friedrich. Biodistribution of charged poly (N-2-(hydroxypropyl)-methacrylamide in tumor bearing rats. *Proc. Int. Symp. Control. Rel. Bioact. Mater.* **28**:1346–1347 (2001).
24. L. W. Seymour, R. Duncan, J. Strohalm, and J. Kopecek. Effect of molecular weight ($M_w$) of N-(2-hydroxypropyl)methacrylamide copolymers on body distribution and rate of excretion after subcutaneous, intraperitoneal and intravenous administration to rats. *J. Biomed. Mater. Res.* **21**:1341–1358 (1987).
25. D. R. Vera, A. M. Wallace, and C. K. Hok. (99mTc)MAG3-mannosyl dextran: a receptor-binding radiopharmaceutical for sentinel node detection. *Nucl. Med. Biol.* **28**:493–498 (2001).
26. D. M. McDonald and P. L. Choyke. Imaging of angiogenesis: from microscope to clinic. *Nat. Med.* **9**:713–725 (2003).
27. R. Satchi-Fainaro. Targeting tumor vasculature: reality or a dream. *J. Drug Target.* **10**:529–533 (2002).